Molecular Therapy
Original Article

Functional restoration of a *CFTR* splicing mutation through RNA delivery of CRISPR adenine base editor

Simone Amistadi,[1,7] Giulia Maule,[1,7] Matteo Ciciani,[1] Marjolein M. Ensinck,[2] Liesbeth De Keersmaecker,[2] Anabela S. Ramalho,[3] Daniela Guidone,[4] Martina Buccirossi,[4] Luis J.V. Galietta,[4,5] Marianne S. Carlon,[2,6] and Anna Cereseto[1]

[1]University of Trento, Department of Computational, Cellular and Integrative Biology, Laboratory of Molecular Virology, 38123 Trento, Italy; [2]KU Leuven, Department of Pharmaceutical and Pharmacological Sciences, Laboratory for Molecular Virology and Gene Therapy, 3000 Leuven, Belgium; [3]CF Research Lab, Woman and Child Unit, Department of Development and Regeneration, KU Leuven, 3000 Leuven, Belgium; [4]Telethon Institute of Genetics and Medicine, 80078 Pozzuoli, Italy; [5]Department of Translational Medical Sciences, University of Napoli "Federico II," 80138 Napoli, Italy; [6]KU Leuven, Department of Chronic Diseases and Metabolism, BREATHE Laboratory, 3000 Leuven, Belgium

Cystic fibrosis (CF) is a genetic disease caused by mutations in the CF transmembrane conductance regulator (CFTR) gene. The 2789+5G>A CFTR mutation is a quite frequent defect causing an aberrant splicing and a non-functional CFTR protein. Here we used a CRISPR adenine base editing (ABE) approach to correct the mutation in the absence of DNA double-strand breaks (DSB). To select the strategy, we developed a minigene cellular model reproducing the 2789+5G>A splicing defect. We obtained up to 70% editing in the minigene model by adapting the ABE to the PAM sequence optimal for targeting 2789+5G>A with a SpCas9-NG (NG-ABE). Nonetheless, the on-target base correction was accompanied by secondary (bystander) A-to-G conversions in nearby nucleotides, which affected the wild-type CFTR splicing. To decrease the bystander edits, we used a specific ABE (NG-ABEmax), which was delivered as mRNA. The NG-ABEmax RNA approach was validated in patient-derived rectal organoids and bronchial epithelial cells showing sufficient gene correction to recover the CFTR function. Finally, in-depth sequencing revealed high editing precision genome-wide and allele-specific correction. Here we report the development of a base editing strategy to precisely repair the 2789+5G>A mutation resulting in restoration of the CFTR function, while reducing bystander and off-target activities.

INTRODUCTION

Cystic fibrosis (CF) is an autosomal recessive monogenic disease caused by mutations in the *CFTR* gene, affecting at least 100,000 people worldwide.[1,2] Several treatments and different drugs, defined as CFTR modulators, are currently used to improve patients' quality of life, but these therapies, while effective, can be extremely costly, associated with side effects, and do not provide a definitive cure. Most importantly, CFTR modulators are not effective with several types of CF-causing mutations.[3–7] Thanks to the early discovery of the *CFTR* gene and associated mutations causing CF, several gene therapy clinical trials have been attempted by delivering the correct gene to compensate for the genetic defect.[8–13]

The delivery of the *CFTR* cDNA through chromatin integration vectors[8,13] or episomal viral/non-viral systems[8–12] offers the opportunity to design a curative strategy valid for any type of mutation.[8–13] More recently, the advancement of genome editing technologies opened the opportunity to permanently correct the genetic defect within the genomic locus, as opposed to the delivery of an exogenous DNA sequence. Since the discovery of CRISPR-Cas9 as an efficient tool for genome editing, several approaches have been developed to repair *CFTR* defects. The reported strategies were based on CRISPR-Cas nuclease activity to generate DSBs for gene substitution through homology directed repair (HDR)[14–19] or deletion of the *CFTR* mutation.[20,21] Nonetheless, even if these methods are promising in repairing the genetic alterations, they might be associated with unwanted genomic rearrangements as consequence of DSBs.[22–26] To overcome this limitation, new CRISPR tools have been developed to modify the genome in the absence of DSBs.[27–29] In this study, we exploited a DSB-free technology, the CRISPR base editor, which consists of a nickase version of Cas9 fused with a DNA deaminase enzyme (an adenine or a cytosine deaminase) determining A>G or C>T transitions.

Received 4 November 2022; accepted 3 March 2023;
https://doi.org/10.1016/j.ymthe.2023.03.004.

[7]These authors contributed equally

Correspondence: Giulia Maule, University of Trento, Department of Computational, Cellular and Integrative Biology, Laboratory of Molecular Virology, 38123 Trento, Italy.
E-mail: giulia.maule@unitn.it
Correspondence: Anna Cereseto, University of Trento, Department of Computational, Cellular and Integrative Biology, Laboratory of Molecular Virology, 38123 Trento, Italy.
E-mail: anna.cereseto@unitn.it

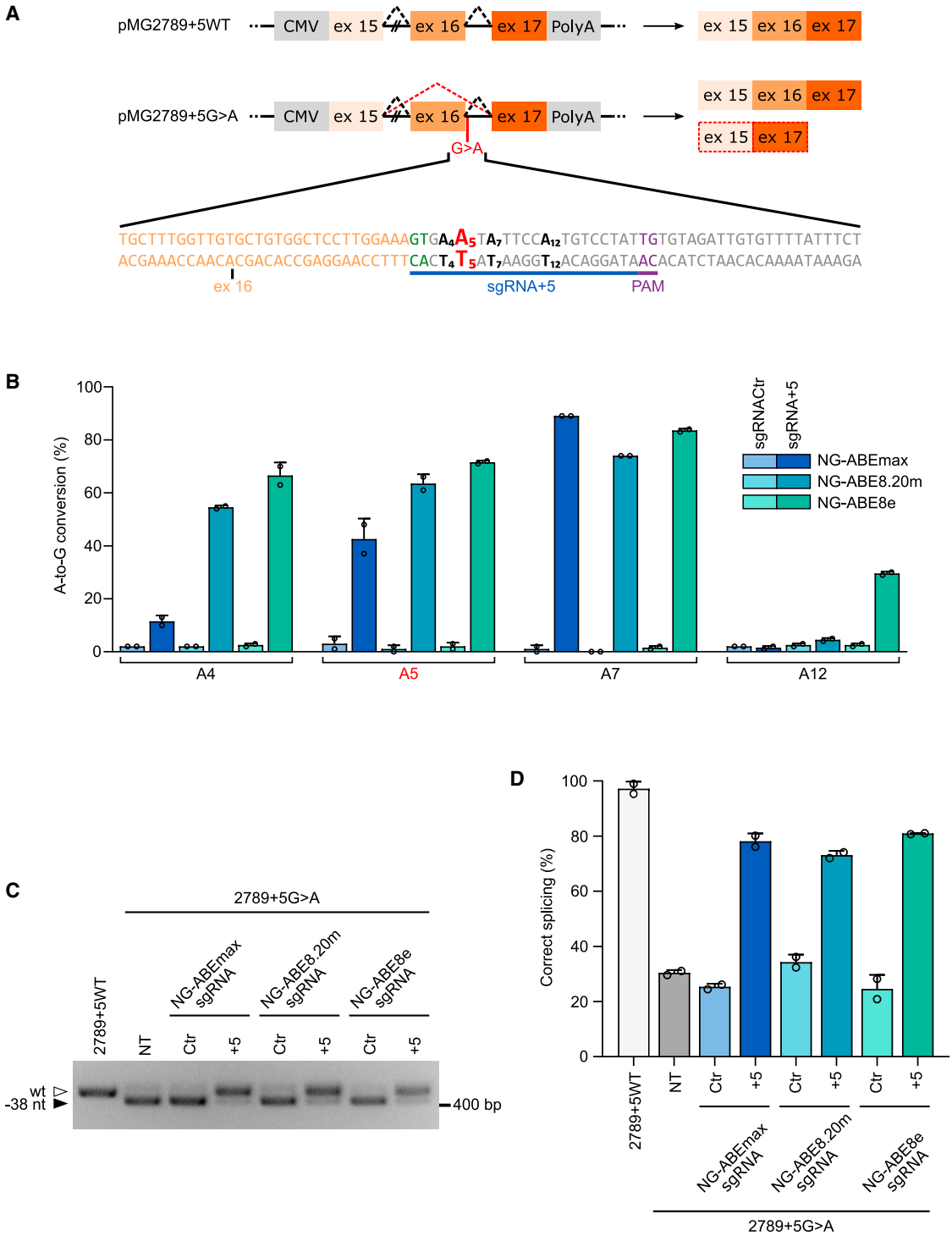

Figure 1. Splicing correction in *CFTR* 2789+5G>A minigene model by adenine base editors

(A) Scheme of the minigene constructs corresponding to *CFTR* gene region from exon 15 to exon 17. Exons depicted as boxes are linked together by introns represented as solid lines. Black dashed lines represent correct splicing, while red lines the aberrant splicing. The constructs are under the expression of the cytomegalovirus (CMV) promoter and terminate with the polyadenylation (poly(A)) signal. The expected splicing products are shown on the right according to the presence or absence of the 2789+5G>A mutation. Below, the nucleotide sequence around the mutation (highlighted in red), the target sgRNA position (underlined, with the PAM in purple), and the conserved GT dinucleotide of the 5′ splice site (in green) is shown. Additional adenines in the typical activity window of the base editor are represented in bold. (B) Editing efficiency measured

(legend continued on next page)

The CFTR2 database lists around 400 variants as CF-causing mutations,[30] 66% accounts for point mutations, of which 46% could be potentially corrected with adenine base editors (ABE) and 15% with cytidine base editors (CBEs).[30,31] Recently, ABE has been applied to target *CFTR* nonsense mutations (R553X, R785X, R1162X, and W1282X) and a splicing mutation (3849+10kbC>T) showing encouraging results of CFTR functional recovery in cell line models, intestinal organoids, or primary epithelial cells.[32–34]

The 2789+5G>A (c.2657+5G>A) *CFTR* mutation is among the 15 most frequent mutations identified to cause CF (∼0.8% of alleles in CFTR2 database).[30] The G-to-A substitution at the +5 position of the splice donor site in intron 16 causes an aberrant splicing with the deletion of exon 16 (38 bp long) from the mature *CFTR* mRNA, eventually leading to an out-of-frame truncated product during translation.[35,36] The base mutation is adjacent to the intron-exon junction and thus not compatible with the use of a conventional CRISPR-Cas9 nuclease approach, which, by generating diverse indel lengths, may alter the near exon sequence.

Here we developed a DSB-free CRISPR strategy through ABE to correct the 2789+5G>A mutation. A critical step to obtain a precise editing was the transient delivery of the ABE RNA as opposed to the long-term expression obtained with a viral vector delivery. By choosing the most precise and efficient method, we showed recovery of CFTR function in patient-derived experimental models, thus setting the groundwork for future clinical development.

RESULTS

Splicing correction of a CFTR 2789+5G>A minigene model

Minigene constructs are useful experimental models to study the splicing process and its regulation by *cis* elements and *trans*-acting factors.[37] To study the CF defects caused by splicing mutations, minigenes were previously reported consisting of portions of *CFTR* exons and introns surrounding the altered site.[38] Similarly, to establish a genome editing strategy, we generated a minigene model mimicking the splicing defect caused by the 2789+5G>A mutation. The constructs included *CFTR* exons 15, 16, and 17, a portion of intron 15, and full-length intron 16, either with the wild-type (pMG2789+5WT) or the mutated (pMG2789+5G>A) sequences (Figure 1A). The splicing pattern produced by the minigene models was validated by RT-PCR and sequencing analysis in transiently transfected HEK293T cells (Figures S1A and S1B). To correct the 2789+5G>A *CFTR* mutation through a base editing approach, we substituted SpCas9 with Cas9-NG in the base editor constructs to exploit the most appropriate ABE editing window targeting the mutation. We tested diverse versions of NG-ABE including NG-ABEmax, NG-ABE8.20m, and NG-ABE8e in combination with two single guide RNAs (sgRNAs), sgRNA+3 or sgRNA+5 (numbered based on the position of the targeted adenine within the spacer sequence), compatible with the targeted mutation. In HEK293 cells stably expressing the 2789+5G>A minigene (HEK293/MG2789+5G>A), the editing efficacy was measured through sequencing and EditR analysis (edit deconvolution by inference of traces in R).[39] All tested ABEs induced variable levels of A-to-G conversions of the mutated adenine (A5) with highest efficiency obtained with the sgRNA+5, resulting in ∼40% editing in combination with either ABE8.20m or ABE8e (Figure S1C). The analysis of the splicing events confirmed that sgRNA+5 in combination with all the NG-ABE constructs had higher efficacy than the sgRNA+3 in restoring the correct splicing pattern (Figure S1D). The sgRNA+5 and three ABE variants (NG-ABEmax, NG-ABE8.20m, and NG-ABE8e) were then tested by lentiviral transduction through an all-in-one vector. The editing efficiency increased to 40%–70% of A-to-G conversion of the mutated adenine (A5) (Figure 1B). As observed in transfection experiments (Figure S1C), we detected relevant bystander activities of intronic adenines in position 4, 7, and 12 (Figure 1B). The splicing analysis revealed a strong correction of the splicing pattern (up to 80% of correctly spliced transcripts) (Figures 1C and 1D), which was confirmed by sequencing of the splicing RT-PCR products (Figures S2A and S2B). The recovery of the proper splicing in the minigene model and the absence of major alteration by sequencing analysis indicated the efficacy of the editing strategy on the 2789+5G>A mutation by the three ABE designs and no detrimental effects of the bystander activity.

Repair of the 2789+5G>A mutation in human rectal organoids

Rectal organoids derived from CF patients are well-established experimental models to test CFTR channel activity.[14,40–43] We evaluated the efficacy of the base editing strategy in organoids derived from a patient compound heterozygous for the 2789+5G>A mutation (2789+5G>A/G542X) through all-in-one lentiviral vector transduction of the ABEs-sgRNA+5. Sequencing of non-treated (NT) organoids and control conditions showed in the A5 position an allelic balance of G/A nucleotides coming from the G542X and 2789+5G>A alleles, respectively (∼50% of total G in position 5). All samples transduced with different ABEs showed ∼10% of A-to-G conversions on the target adenine (editing reported as G% above the NT and control conditions) (Figures 2A, S3A, and S3B). Bystander activity was detected on the adjacent adenines; in particular, A7 was targeted by all the base editors, while A4 was mainly modified by NG-ABE8.20m and NG-ABE8e (Figure 2A). The splicing analysis of NT and control organoids showed an altered transcript produced by exon 16 skipping together with wild-type mRNAs deriving from the G542X allele and partly from the 2789+5G>A allele (Figure 2B). We observed a significant increase of the correct splicing products with all the tested ABEs and in particular with NG-ABEmax-sgRNA+5 (almost ∼75% of correctly spliced products) (Figure 2C). The *CFTR* gene repair and the recovery of the ion

by EditR tool[39] using Sanger sequencing chromatograms from HEK293/2789+5G>A cells transduced with lentiviral vectors expressing NG-ABEmax, NG-ABE8.20m, and NG-ABE8e with either a control sgRNA (sgRNACtr) or sgRNA+5. The mutation (A5) is reported in red; bystander adenines are in black. (C) Representative RT-PCR products and (D) percentages of correct splicing measured by densitometry obtained from cells treated as in (B). HEK293 stably expressing pMG2789+5WT was used as a reference for correct splicing. White empty arrow indicates correct splicing, black solid arrow indicates aberrant splicing. Data are means ± SD from n = 2 independent experiments.

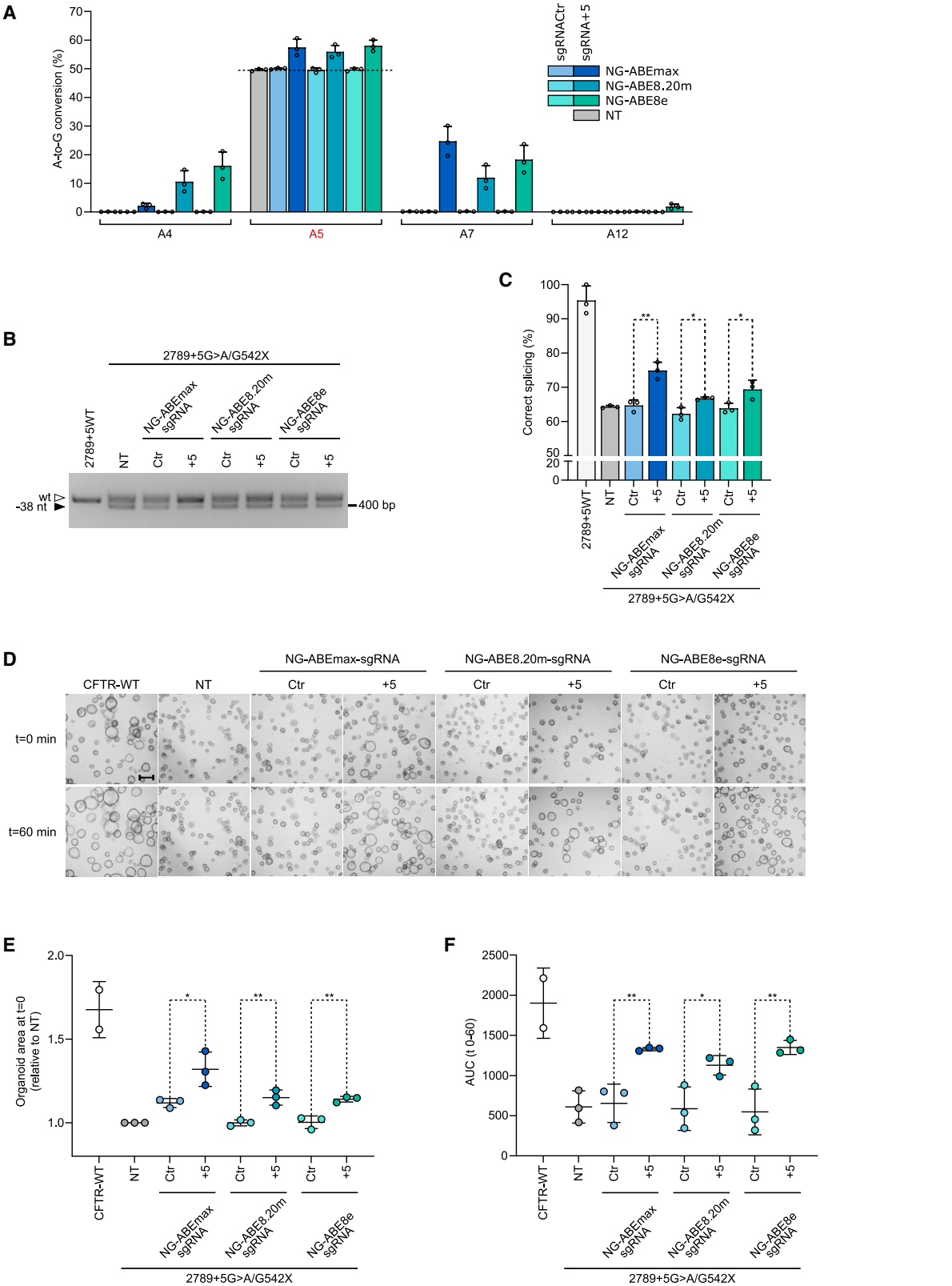

(legend on next page)

channel function was evaluated after ABEs-sgRNA+5 transduction versus control treatment. Specifically, CFTR activity is tightly correlated with an increase in the organoid area (swelling) as a result of anion and fluid secretion into the organoid lumen.[40] The presence of the nonsense G542X mutation on the second allele, producing no CFTR protein, is an ideal genetic context as all the functional correction will derive from the 2789+5G>A allele. Two weeks after transduction, we observed a significant increase in organoid area at steady state in the ABEs-sgRNA+5-treated organoids compared with the controls (Figures 2D and 2E), with ABEmax as best performing, consistently with the degree of splicing correction. As reported in former studies,[21,32] the size of the organoids was heterogeneous, likely due to the formation of organoids containing variable amounts of edited cells. CFTR function was also measured through forskolin-induced swelling (FIS) assay,[40] further confirming the restored CFTR activity following ABE treatment (Figure 2F).

To investigate whether the bystander edits of the adenines surrounding the mutation potentially alter the 5′ splice recognition site in intron 16, we created minigene models recapitulating all the possible editing outcomes generated by unwanted editing. The analysis of the transcripts generated by the mutated minigenes revealed that the conversion of the adenine in position 7 (A7) into a guanine had no visible impact on the splicing pattern. Conversely, a guanine in position 4 (A4) resulted in a detectable transcript alteration, likely due to skipping of exon 16 (Figure S4A). This observation was further confirmed by *in silico* analysis through MaxEnt,[44] which showed that this substitution decreased the strength of the splice site (Figure S4B). These results were consistent with reduced splicing correction in organoids treated with NG-ABE8.20m and NG-ABE8e, in which, despite similar editing activity on the mutated adenine A5, the additional editing of A4 diminished the splicing correction (Figure 2A). Therefore, the NG-ABEmax efficacy on the targeted 2789+5G>A mutation was likely tempered by the limited bystander activity in the near adenine A4.

RNA delivery of base editor corrects the 2789+5G>A mutation in rectal organoids

Given the efficacy of the NG-ABEmax-sgRNA+5 approach, we set to limit the associated bystander editing, which we have shown counteracting the on-target efficacy. It has been reported that non-specific editing can be reduced through transient expression of the CRISPR-Cas system.[45,46] We then chose to deliver the base editor and the sgRNA as RNA. The RNA delivery of *in vitro* transcribed NG-ABEmax mRNA and the synthetic sgRNA was initially tested in HEK293/MG2789+5G>A, where we observed 10% conversion of the mutated adenine in the minigene sequence with a minimal amount of unwanted A4 editing (Figure S5A). We then tested the editing using RNA delivery through electroporation in rectal organoids compound heterozygous for the 2789+5G>A mutation. We reached approximately 5% of A-to-G conversion of the mutated adenine (Figures 3A and S5B) and low editing on the adjacent A4 (0.8% of total reads) (Figure 3A). Therefore, even though the electroporation resulted in decreased editing efficiency compared with lentiviral transduction, which is consistent with lowered efficiency of nucleic acid delivery (Figures S6A and S6B), the bystander A4 edit was better controlled (Figure S5C). To evaluate whether the percentage of specific editing was sufficient to sustain the correct splicing, we analyzed the splicing profile, which showed an increase of correct transcripts (~75% of wild-type transcripts in edited organoids) (Figures 3B and S5D). To finally evaluate the CFTR recovery obtained through the RNA delivery of NG-ABEmax-sgRNA+5, we measured the organoid area 2 weeks after the treatment either at steady state or through the FIS method. The results showed a significant increase in organoid area in the NG-ABEmax-sgRNA+5 condition compared with the controls at the steady state and after the FIS assay, confirming a functional restoration of the CFTR channel activity (Figures 3C and 3D). In conclusion, RNA delivery of NG-ABEmax-sgRNA+5 restored the CFTR functionality in patient-derived models carrying the 2789+5G>A mutation.

Functional recovery of the CFTR anion transport in primary bronchial epithelial cells

To thoroughly evaluate the base editing efficacy in relevant CF experimental models, we measured the electrophysiological properties of edited primary bronchial epithelial (BE) cells obtained from an individual carrying the 2789+5G>A mutation and the F508del. Electroporation of BE cells with base editor mRNA and sgRNA produced 5% of base conversion at the A5 target site (Figure 4A), consistent with the rectal organoid results (Figure 3A). Here the bystander editing of A7 was approximately 20%, while lower A4 modification was revealed (3%) (Figures 4A and S7A). BE cells were then cultured under air-liquid interface (ALI) conditions generating a multi-ciliated pseudostratified epithelium that recapitulates the ion transport mechanisms of the airway epithelium *in vivo*.[47,48] After 2–3 weeks of ALI culture, we measured the short-circuit current intensity (Isc). After blocking ENaC (epithelial sodium channel) activity with amiloride, CFTR-dependent chloride secretion was stimulated with the membrane-permeable cyclic AMP (cAMP) analog 8-(4-chlorophenylthio) adenosine 3′,5′-cyclic monophosphate (CPT-cAMP) and then blocked with

Figure 2. Functional correction of CFTR in 2789+5G>A rectal organoids

(A) Percentage of A-to-G conversions of target adenines measured by targeted deep sequencing in rectal organoids (2789+5G>A/G542X) 14 days after lentiviral transduction with NG-ABEmax, NG-ABE8.20m, and NG-ABE8e with either a control sgRNA (sgRNACtr) or sgRNA+5. Non-treated (NT) organoids were used as an additional control. The dashed line indicates the baseline %G in NT cells. (B) Representative image of splicing pattern analysis by RT-PCR in organoids treated as in (A). (C) Percentages of correctly spliced transcripts measured by densitometry. Data are means ± SD from n = 3 independent experiments. (D) Representative images of rectal organoids before (t = 0 min) and after (t = 60 min) FIS assay (0.8 μM forskolin). The positive control (CFTR-WT) used corresponds to the rectal organoids (2789+5G>A/G542X) treated with a lentiviral vector carrying WT-CFTR cDNA. Scale bar, 200 μm. (E) Quantification of organoid area at time = 0 min and (F) fold change following FIS assay over 60 min of organoids transduced as in (A). Each dot represents the average of eight wells (number of organoids per well: 100–300) from n = 3 independent experiments. Data are presented as means ± SD. Statistical analyses were performed using unpaired t test comparing sgRNACtr versus sgRNA+5 conditions with the different ABEs. *$p < 0.05$; **$p < 0.01$; n.s., non-significant.

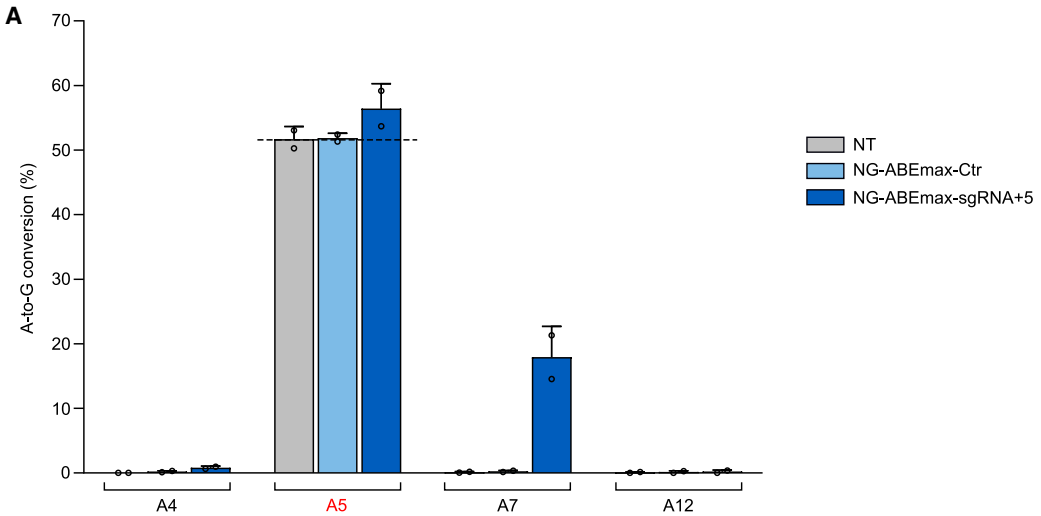

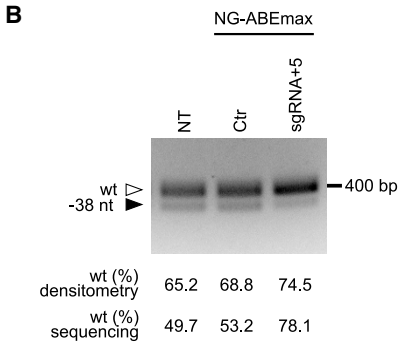

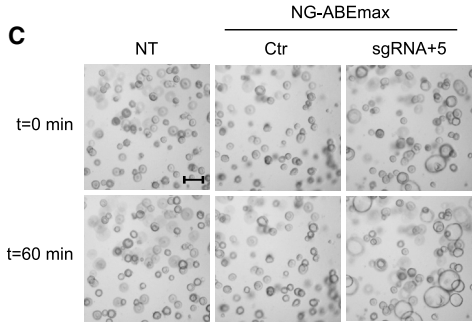

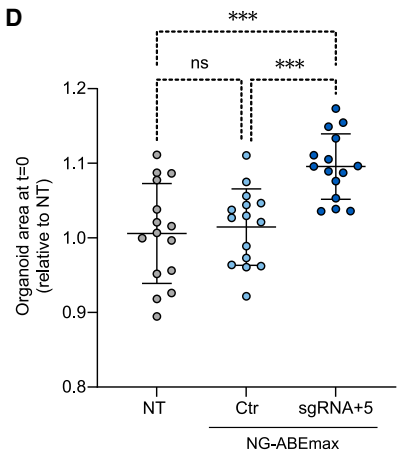

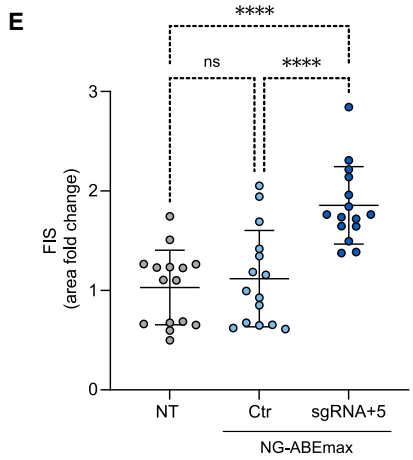

(legend on next page)

$CFTR_{inh}$-172 (inh-172) (Figure 4B). The amplitude of inh-172 current drop ($\Delta I_{inh-172}$) was taken as the parameter reflecting CFTR function (Figure 4C). Cells treated with NG-ABEmax-sgRNA+5 showed overall higher CFTR function compared with the NT and the control conditions (Figure 4B). We found a nearly 4-fold increase of $\Delta I_{inh-172}$ in edited cells (Figure 4C), with an absolute value of ~1 μA, which, after normalization for surface unit, corresponds to ~3 μA/cm^2. This value is approximately 13%–18% of the average CFTR activity ($\Delta I_{inh-172}$ = 17–23 μA/cm^2) measured in non-CF epithelia under similar conditions.[48,49] Interestingly, we detected a baseline CFTR activity in the controls, likely due to the residual correct splicing originating from the 2789+5G>A allele and the F508del second allele. We also measured the amplitude of the block elicited by amiloride, which is due to ENaC function. We found no significant change elicited by CFTR gene editing compared with controls (Figure S7B). In conclusion, these results showed that base editing partly rescues the CFTR activity as direct measurement of the anion conductance in primary BE cells.

Editing precision: Allelic discrimination and off-target sites

Given the efficacy of the base editor and sgRNA+5 in restoring the CFTR activity, we then evaluated the levels of editing precision. We first assessed the allelic discrimination of the identified strategy in condition of heterozygosity, most frequently occurring in CF,[50] by verifying the editing specificity on the 2789+5G>A mutation versus the second allele. To this aim, the base editor mRNA and the sgRNA were electroporated into primary BE cells from a non-CF individual to test the modification of a non-2789+5G>A allele. In this context, with the absence of the mutated target A5, we exploited the bystander edits (particularly A4 and A7) to measure the sgRNA+5 specificity. We analyzed the editing through deep sequencing for maximum sensitivity and we detected near background levels of editing in A4 and A7, while a sgRNA fully matching the wild-type allele (sgRNAWT), used as control, showed high percentages of A-to-G conversion of A4 and A7 (~15% and ~65%, respectively) (Figure 5A). Therefore, the NG-ABEmax-sgRNA+5 showed high specificity toward the mutated locus while inducing no modifications of the second heterozygous allele.

To test the off-target activity throughout the genome, we used GUIDE-seq analysis[51] by employing Cas9-NG nuclease and sgRNA+5 to detect sites where modification may occur with the base editor. Off-target sites retrieved by Cas9-NG-sgRNA+5 in HEK293/MG2789+5G>A were very limited in number (n=5), and, for each site, the amounts of cleavages were close to background (Figure S8A). Nonetheless, to further evaluate the editing precision in primary BE cells, we deep sequenced the A-to-G conversions in the off-target sites identified through GUIDE-seq analysis, and two additional sites predicted *in silico* having up to two mismatches. The percentages of A-to-G conversions obtained from the deep sequencing were limited to background levels, including the highly repeated sequence of OT3 where the detectable modifications corresponded to naturally occurring SNPs present also in the control sample (Figure 5B). Overall, these results indicate a high precision both on the second allele and throughout the genome.

DISCUSSION

Gene therapy has been widely explored in CF aiming at compensating the *CFTR* genetic defects through gene complementation approaches.[8–13] However, the advancement of genome editing technologies offers the unprecedented opportunity to correct the endogenous CFTR in order to preserve the genetic regulatory elements surrounding the repaired gene. CRISPR strategies based on Cas nucleases activity have been proved valid to correct common CF genetic alterations, including F508del and splicing mutations (3272-26A>A and 3849+10kbC>T).[14,15,17–21] These editing strategies use cellular repair pathways engaged by DSBs generated by CRISPR-Cas nucleases to introduce modification at specific sites. Emerging data, however, show that DSBs in genome editing are associated with unpredictable genomic alteration, including large deletions and chromosomal loss or translocations.[22–24] As a response to these rising issues, CRISPR technologies have been further developed, aiming at modifying the genome in the absence of DSBs. This is achieved by exploiting functional domains (deaminases or reverse transcriptase) fused to a mutated Cas9 nickase.[27–29] Base editors, made with deaminase domains, have been applied to CF mutations showing functional restoration of intestinal organoids carrying *CFTR* nonsense mutations (R553X, R785X, R1162X, W1282X).[32] In this study, we demonstrated that a CRISPR adenine base editor can be applied to precisely correct the 2789+5G>A mutation, which is one of the most frequent genetic alterations causing aberrant splicing in CF.[30] To determine the most effective and precise base editing strategy, we developed a CF minigene model mimicking the genetic defect expressed in cell lines. To validate the genetic and functional restoration of CFTR, we used patient-derived models consisting of rectal organoids and BE cells grown as multi-ciliated pseudostratified epithelia. To direct the base editing tool to the target site, we first substituted the newly evolved adenine base editors (ABE8e, ABE8.20m, and ABEmax)[52–54] with a Cas9 mutant, Cas9-NG, binding to the best PAM near the 2789+5G>A mutation. This allowed us to obtain high A-to-G

Figure 3. RNA delivery of the NG-ABEmax-sgRNA+5 repairs the CFTR channel in 2789+5G>A rectal organoids

(A) Editing efficiency of rectal organoids 2 weeks after electroporation with NG-ABEmax mRNA either alone (Ctr) or with sgRNA+5. As control NT rectal organoids were electroporated with a control GFP mRNA. A-to-G conversion levels were measured by targeted deep sequencing. The dashed line indicates the baseline %G in NT cells. Data are means ± SD from n = 2 independent experiments. (B) Splicing pattern analysis by RT-PCR in organoids treated as in (A). The black solid arrow indicates aberrant splicing, the white empty arrow indicates correct splicing. The percentage of aberrant splicing (exclusion of 38 nt) was measured by agarose gel densitometry and Sanger sequencing and chromatogram decomposition analysis through the DECODR tool. (C) Representative images of rectal organoids electroporated as in (A) before (t = 0 min) and after (t = 60 min) FIS assay (0.8 μM forskolin). Scale bar, 200 μm. (D) Quantification of organoid area at time = 0 min and (E) area fold change from t = 0 to t = 60 min. Each dot represents the average of one well (number of organoids per well, 100–300) from n = 2 independent experiments. Data are presented as means ± SD. Statistical analyses were performed using one-way ANOVA followed by Tukey's multiple comparison test with a single pooled variance. ***p < 0.001; ****p < 0.0001; n.s., non-significant.

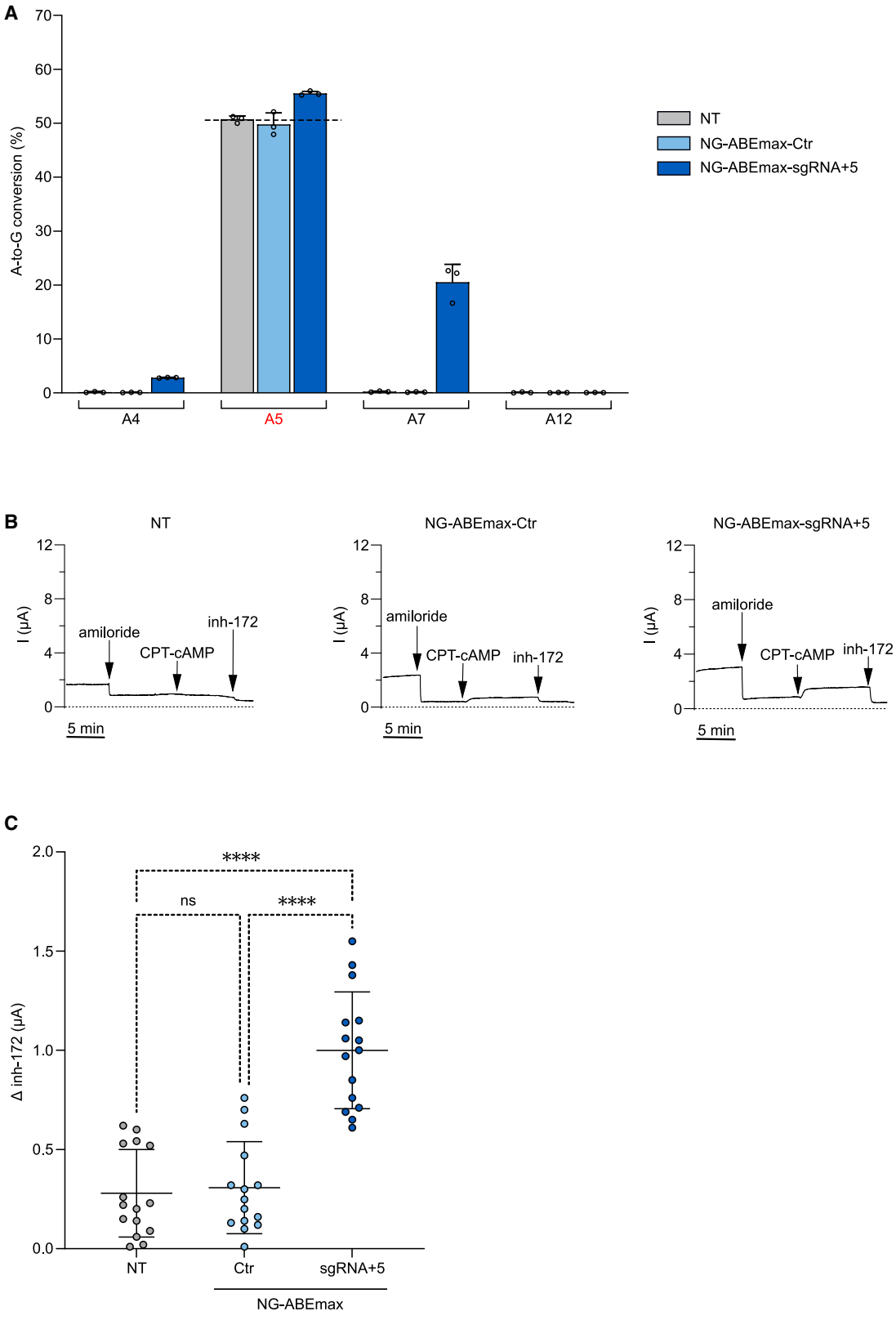

(legend on next page)

conversions at the target nucleotide (up to 70%), which was, however, associated with various grades of bystander edits. A non-trivial caveat in base editing approaches is the window of deamination, which is often larger than the target site, and frequently resulting in nucleotide deamination surrounding the target nucleobase (bystander activity). Even though base editing technology is heavily under development toward the clinic,[55] the bystander edits require a careful evaluation, balancing the benefits over the side effects of the editing strategy. These additional base conversions are particularly relevant if they occur in the coding sequence, as was reported for the W1282X mutation correction.[34] In our work, the bystander activity was occurring in the intronic region, thus limiting the impact of direct protein alterations. However, we discovered that these secondary edits affected the splicing activity, thus at least partially counteracting the repair efficacy of the on-target modification. The first strategy utilized to tackle this problem was the selection of the ABE able to achieve the highest on-target over bystander profile, the ABEmax. The second strategy employed to optimize the editing outcome was the method of delivery. Indeed, in general, the editing outcome highly depends on the transfer technique, which affects the duration of editing activity and the amounts of the modifying enzyme accumulating in the target cells.[56–58] Recent technological advancement on RNA delivery showed advantages of its application in genome editing, including transient expression, which correlates with reduced off-target activity.[45,46] Here we demonstrated that the RNA delivery of the base editor, even though less efficient than the lentiviral delivery, worked both in organoids and BE cells derived from compound heterozygous patients carrying the 2789+5G>A mutation. Compared with viral vector delivery, the bystander activity was reduced together with on-target editing. Nonetheless, while the detrimental effect of the bystander was significantly decreased, the on-target effect was sufficient to generate a functional repair of CFTR in primary cells and organoids. Clonal selection used in similar studies using organoids[32] was not necessary with our approach. Interestingly, similar to previous genome editing studies,[21,34] our data indicated that less-than-complete correction of one allele was sufficient in compound heterozygous organoids and epithelial cells to obtain CFTR recovery. Precise single allele modification is consequently extremely relevant to obtain the highest therapeutic efficacy and prevent potential side effects from bystander edits. Our approach was thoroughly evaluated to exclude second allele editing as well as off-target activities genome-wide. Even though partial single allele correction was sufficient to recover CFTR function both in organoids and in multi-ciliated pseudostratified epithelia, the percentages of cells and cell types needed to be targeted in the airways epithelium to alleviate the respiratory symptoms in people with CF still remain an open question. Several studies and clinical data reported that 10% of CFTR expression should be sufficient to ameliorate clinical manifestations of the disease,[59–62] but more studies using animal models are needed to address open issues in gene therapy.[8]

In conclusion, here we identified a strategy to functionally correct the 2789+5G>A *CFTR* splicing mutation by means of a DSB-free second-generation CRISPR technology, which was validated in primary cell models deriving from patients. Obviously, the nucleofection of dissociated cells to deliver the genome editing technology is a way to bypass the barriers that differentiated epithelia display against intracellular delivery of nucleic acids and proteins. To efficiently deliver the therapeutic macromolecular complexes to differentiated epithelia, very efficient vectors need to be developed. However, our results showed a degree of CFTR correction and editing precision that poses this study as groundwork for further development toward the clinic.

MATERIALS AND METHODS

Plasmids

Wild-type and mutated minigenes for 2789+5G>A mutation were cloned into pcDNA3 plasmid. Wild-type minigene (pMG2789+5WT) was obtained by PCR amplification and cloning of target regions from the *CFTR* gene of HEK293T cells. Oligonucleotides are listed in Table S1. The pMG2789+5WT plasmid contains full exons 15, 16, and 17, portions of intron 15, and full intron 16. Mutated minigene (pMG2789+5G>A) was obtained by site-directed mutagenesis of wild-type minigene constructs. Oligonucleotides are listed in Table S1. The additional minigenes for 2789+5G>A mutation (pMG2789_AG, pMG2789_GG, pMG2789_GGG, pMG2789_GGGG) were obtained by PCR amplification and cloning of target regions from HEK293T cells edited with NG-ABEmax or NG-ABE8e and CFTR 2789 sgRNA+5. Plasmids expressing sgRNAs were constructed by ligation of annealed oligonucleotides into BbsI-digested pUC19-sgRNAopt (pUC19 plasmid with sgRNA cassette derived from pX330, Addgene #42230). Sequences of sgRNAs are reported in Table S2. Transfer vector plasmids (pLentiNG-ABEmax-sgRNACtr, pLentiNG-ABE8.20m-sgRNACtr, pLentiNG-ABE8e-sgRNACtr) were constructed starting from pLenti-FNLS-P2A-Puro plasmid (Addgene #110841) and by replacing BE4max sequence with ABE sequences by plasmid DNA cloning by restriction enzyme digestion. The sgRNA expression cassette was then inserted into XhoI-digested plasmid by using GeneArt Gibson Assembly HiFi kit (Thermo Fisher) following manufacturer's instructions. Plasmids expressing sgRNAs targeting CFTR 2789+5G>A mutation were constructed by ligation of annealed oligonucleotides into BsmBI-digested pLentiNGABE-sgRNACtr. Plasmids expressing NG-ABEmax, NG-ABE8e, and NG-ABE8.20m were cloned by

Figure 4. RNA delivery of the NG-ABEmax-sgRNA+5 functionally restores CFTR activity in primary BE cells derived from a 2789+5G>A patient

(A) Editing efficiency analyzed by targeted deep sequencing in primary BE cells (2789+5G>A/F508del) 3 days after electroporation of NG-ABEmax mRNA either alone (Ctr) or with sgRNA+5. Data are means ± SD from n = 3 independent experiments. (B) Representative short-circuit current traces measured on ALI epithelia of NT or NG-ABEmax-Ctr and NG-ABEmax-sgRNA+5 treated cells. (C) CFTR anion channel activity represented as amplitude of $CFTR_{inh}$-172 effect. Dots represent the results from epithelia of n = 3 independent experiments. Data are presented as means ± SD. For each experiment, four to six ALI cultures were prepared. Statistical analyses were performed using one-way ANOVA followed by Tukey's multiple comparison test. ****$p < 0.0001$; n.s., non-significant.

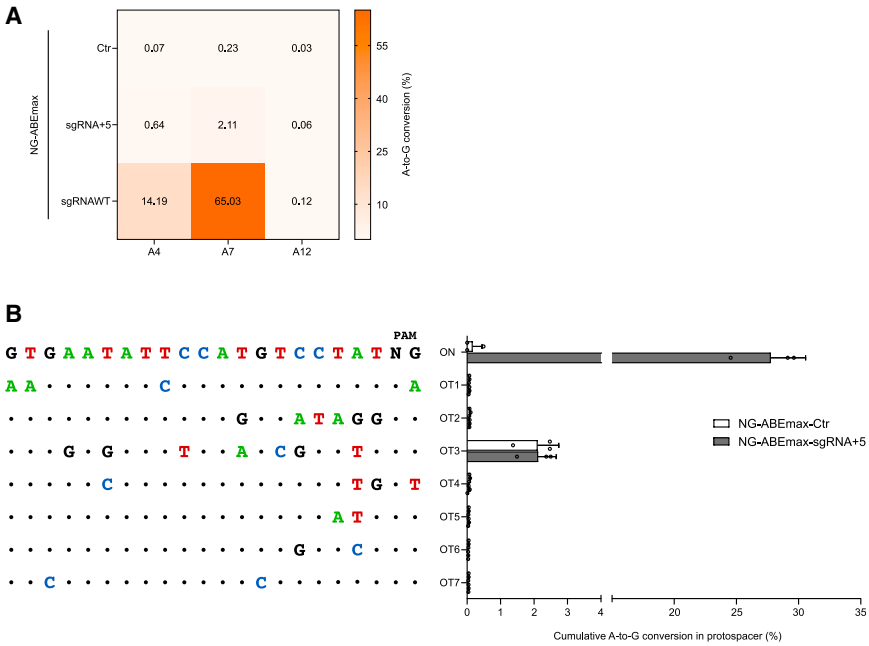

Figure 5. Specificity of the base editing approach in primary BE cells

(A) A-to-G conversions measured by targeted deep sequencing in primary BE cells from a non-CF individual. Cells were electroporated with NG-ABEmax mRNA alone (Ctr), with sgRNA+5 specific for the 2789+5G>A mutation, or an sgRNA fully matching the WT-*CFTR* sequence (sgRNAWT). Data are means from n = 3 independent experiments. (B) Deep-sequencing analysis performed on off-target sites identified through GUIDE-seq analysis (OT1-OT5) and predicted *in silico* based on sequence homology (OT6, OT7). Cumulative A-to-G base conversions of adenines inside the sgRNA spacer is reported for cells treated with NG-ABEmax RNA either alone (Ctr) or in combination with sgRNA+5. Data are means ± SD from n = 3 independent experiments.

substituting in pCMV-ABEmax plasmid (Addgene #112095) the sequence of NG-ABEmax and sequences described for ABE8e and ABE8.20m[53,54] fused to Cas9-NG sequence. Oligonucleotides used in PCR amplifications are listed in Table S3.

Cell lines

HEK293T, HEK293, and HEK293 cells stably expressing pMG2789+5-WT (HEK293/MG2789+5WT), and pMG2789+5G>A (HEK293/MG2789+5G>A), were cultured in Dulbecco's modified Eagle's medium (DMEM; Life Technologies) supplemented with 10% fetal bovine serum (FBS; Life Technologies), 10 U/mL antibiotics (PenStrep; Life Technologies), and 2 mM L-glutamine at 37°C in a 5% CO_2 humidified atmosphere. HEK293T and HEK293 cells were obtained from the American Type Culture Collection (ATCC; www.atcc.org).

Stable minigene cell lines were produced by transfection of BglII-linearized minigene plasmids (pMG2789+5WT, pMG2789+5G>A) in HEK293 cells. Cells were selected with 500 μg/mL of G418 (Thermo Fisher) 72 h after transfection.

Transfection and lentiviral transduction of cell lines

HEK293/MG2789+5G>A were seeded in a 24-well plate and transfected with TransIT-LT1 (Mirus) according to manufacturer's protocol with 750 ng of plasmid encoding for CRISPR base editor and 250 ng of plasmid encoding for sgRNA. Cells were collected 10 days after transfection to perform editing efficiency and transcripts analyses.

Lentiviral particles were produced in HEK293T cells seeded at 80% confluency in 10-cm plates, and 10 μg of transfer vector (pLentiNG-ABEmax-sgRNA) plasmid, 3.5 μg of VSV-G, and 6.5 μg of Δ8.91 packaging plasmid were transfected using polyethylenimine (PEI). After overnight incubation, the medium was replaced with complete DMEM. The viral supernatant was collected after 48 h, centrifuged to eliminate cellular debris, and filtered in a 0.45 μm filter. Lentiviral particles were concentrated and purified with 20% sucrose cushion by ultracentrifugation for 2 h at 4°C and 150,000 × *g*. Pellets were resuspended in an appropriate volume of OptiMEM. Aliquots were stored at −80°C. Vector concentration was measured as reverse transcriptase units (RTU) by SG-PERT method.[63]

For transduction experiments, HEK293/MG2789+5G>A were seeded in a 24-well plate (150,000 cells/well) and transduced with either 1 RTU or 0.2 RTU of lentiviral vectors. Forty-eight hours later, cells were selected with puromycin (1 μg/mL) and collected 10 days after selection for editing efficiency and transcripts analyses.

Editing efficiency analysis

Genomic DNA was extracted using QuickExtract DNA extraction solution (Epicentre). Target regions were amplified by PCR with Phusion High Fidelity DNA Polymerase (Thermo Fisher) using 100–500 ng of DNA as template. Oligos are listed in Table S1. PCR products were purified using NucleoSpin Gel and PCR Clean-up (Macherey-Nagel) and sequenced by Sanger sequencing. To evaluate editing efficiency, the chromatograms were analyzed using EditR software.[39]

Transcripts analysis

RNA was extracted either using TRIzol Reagent (Invitrogen) or NucleoSpin RNA kit (Macherey-Nagel) following manufacturer's instructions and resuspended in DEPC-double-distilled H_2O (ddH_2O). cDNA was obtained starting from 100 to 500 ng of RNA using RevertAid Reverse Transcriptase (Thermo Scientific) according to the manufacturer's protocol. Target regions were amplified by PCR with Phusion High Fidelity DNA Polymerase (Thermo Fisher). Oligonucleotides are listed in Table S1. The different splicing products

were quantified by densitometry analysis of agarose gel or DECODR[64] analysis of Sanger sequenced PCR products.

In silico splicing prediction

Wild-type, mutated, and edited *CFTR* gene sequences were analyzed with the MaxEntScan::score5ss for human 5′ splice sites[44] based on the maximum entropy principle (http://hollywood.mit.edu/burgelab/maxent/Xmaxentscan_scoreseq.html).

In vitro mRNA transcription

NG-ABEmax mRNA was synthesized by T7 polymerase *in vitro* transcription using MEGAScript T7 (Invitrogen) and following manufacturer's protocol. In detail, 500 ng of linearized NG-ABEmax-P2A-GFP plasmid (Addgene #140005) were used as template for the reaction. GTP was substituted with a 4:1 mix of anti-reverse cap analog (ARCA) and GTP. The Poly(A) Tailing Kit (Invitrogen) was used to add the poly(A) tail on the mRNA following the manufacturer's instructions. The mRNA was purified with LiCl precipitation and resuspended in DEPC-ddH_2O. The sgRNA+5 was synthetically ordered and produced from Integrated DNA technologies (IDT) (Alt-R CRISPR-Cas9 sgRNA).

Electroporation of cell lines

Two-hundred thousand HEK293/MG2789+5G>A cells were electroporated with the Amaxa 4D-Nucleofector (SE Cell Line buffer, CM-130 program) and seeded into a 12-well plate, and 3 μg of base-editor mRNA either alone (Ctr) or with 3 μg of sgRNA+5 were used for the electroporation. Cells were collected after 3 days for editing analysis.

GUIDE-seq

GUIDE-seq experiments were performed as described in previous studies.[51,65] Briefly, HEK293/MG2789+5G>A cells were transfected using Lipofectamine 3000 transfection reagent (Invitrogen) with 500 ng of Cas9-NG plasmid, 250 ng of CFTR 2789 sgRNA+5 plasmid, and 10 pmol of dsODNs. Twenty-four hours after transfection, cells were detached and selected with 1 μg/mL puromycin. Four days after transfection, cells were collected and genomic DNA was extracted using DNeasy Blood and Tissue kit (Qiagen) following manufacturer's instructions. Genomic DNA was sheared to an average length of 500 bp using a focused ultrasonicator (Covaris). End-repair reaction was performed using NEBNext Ultra End Repair/dA Tailing Module and adaptor ligation using NEBNext Ultra Ligation Module, as described by Nobles et al.[65] Amplification steps were then performed following the GUIDE-seq protocol from Tsai et al.[51] Following quantification of the libraries by Qubit dsDNA High Sensitivity Assay kit (Invitrogen), MiSeq sequencing system (Illumina) was used with an Illumina Miseq Reagent kit V2-150PE. Raw sequencing data (FASTQ files) were analyzed using the GUIDE-seq computational pipeline available at https://github.com/tsailabSJ/guideseq. GUIDE-seq data are available in Table S6.

In silico off-target analysis

Off-target sites for sgRNA+5 were analyzed by Cas-OFFinder online algorithm[66] by selecting: XCas9 3.7 (TLIKDIV SpCas9) from *Streptococcus pyogenes* 5′-NG-3, mismatch number ≤ 4, DNA bulge size = 0, and as a target genome the *Homo sapiens* (GRCh38/hg38), human. Full analysis results are available in Table S5.

Targeted deep sequencing

Genomic DNA was extracted from human intestinal organoids (2789+5G>A/G542X) 14 days after the treatment and from human CF (2789+5G>A/F508del) or non-CF primary BE cells 3 days after electroporation. The loci of interest (on and off targets) were amplified using Phusion high-fidelity polymerase (Thermo Scientific). Amplicons were indexed by PCR using Nextera indexes (Illumina), quantified with the Qubit dsDNA High Sensitivity Assay kit (Invitrogen), pooled in near-equimolar concentrations, and sequenced on an Illumina Miseq system using an Illumina Miseq Reagent kit V2−300 cycles (2 × 150 bp paired end). Primers used for PCR amplification are listed in Table S4. FASTQ data were analyzed using CRISPResso online tool[67] by selecting base editors as editing tool, minimum homology for alignment = 60%, base editor output A>G, quantification window centered −10 (relative to the 3′ end of the sgRNA), and window size = 10.

The percentage of G nucleotide in the adenines present in the protospacer was considered as editing. The results of CRISPResso analysis are presented in Table S7.

Human rectal organoids culture

Human rectal organoids of a CF subject compound heterozygous for the 2789+5G>A splicing mutation (2789+5G>A/G542X, n=1) were generated and cultured as described previously.[68] The Ethics Committee of the University Hospital Leuven approved this study and informed consent was obtained from all participating CF subjects. Lentiviral vector transduction of human rectal organoids was performed as described previously.[41] Briefly, organoids were trypsinized to single cells and resuspended with the viral vector and Matrigel and plated. For nucleofection of human rectal organoids, cells were trypsinized to single cells. Then 120,000 cells were resuspended in the Human Stem Cell Nucleofector kit 2 solution (Lonza) with 6 μg of base editor mRNA either alone (Ctr) or with 6 μg of sgRNA (Alt-R CRISPR-Cas9 sgRNA, IDT). Cells were then placed in the Amaxa nucleofector I and after nucleofection, Matrigel was added, and the cells were plated. For both lentiviral vector and nucleofection, cells were incubated for approximately 2 weeks to allow formation and growth of organoids in complete medium,[68] which was supplemented with Y-27632 for the first 3 days.

Analysis of CFTR activity in intestinal organoids

Fourteen days after viral vector transduction or electroporation, correction of CFTR function was evaluated by the FIS assay, as described previously.[42] Briefly, 5× brightfield images were taken before the start of the assay (t = 0), after which the organoids were treated with 0.8 μM forskolin and images were taken every 10 min for the next hour. Images were exported to ImageJ and analyzed with a custom macro that creates a mask of the area of the organoids at each time point. Relative organoid swelling was analyzed in

Microsoft Excel, and the resulting area under the curve (AUC) between t=0 and t=60 was calculated in GraphPad Prism 9.

Primary BE cell culture

Primary airway BE cells were derived from a CF patient compound heterozygous for the 2789+5G>A splicing mutation (2789+5G>A/F508del, n=1) (kindly provided by the Primary Cell Culture Service of the Italian Cystic Fibrosis Research Foundation). The Ethics Committee of the Istituto Giannina Gaslini approved this study and informed consent was obtained from all participating CF subjects. Cells were cultured in LHC9/RPMI 1640 (1:1) without serum as previously described,[47,48] supplemented with rho-associated protein kinase 1 inhibitor (Y-27632, 5 μM) (Merck) and SMAD-signaling inhibitors, bone morphogenetic protein antagonist (DMH-1, 1 μM), and transforming growth factor β antagonist (A 83-01, 1 μM), to promote basal cell proliferation as previously reported.[69] At passage 3, 200,000 cells were electroporated with the Amaxa 4D-Nucleofector (P3 primary cells buffer, DN-100 program) and seeded into a six-well plate previously treated with collagen. Electroporation was performed with 3 μg of base editor mRNA either alone (Ctr) or with 3 μg of sgRNA (Alt-R CRISPR-Cas9 sgRNA, IDT). Part of the cells were collected for editing analysis after 3 days, and the remaining were seeded at high density on Transwell (cc3470, Corning Costar; 0.33 cm^2 surface) porous inserts (150,000 cells per insert). After 24 h, the proliferative medium on the basolateral side was replaced with differentiation medium PneumaCult ALI (Stemcell Technologies), whereas the medium on the apical side was totally removed to obtain the ALI condition. Short-circuit current experiments were performed after 2–3 weeks in culture, when epithelia achieved full mucociliary differentiation.

Short-circuit current recordings

Transwell supports carrying differentiated bronchial epithelia were mounted in an Ussing-like vertical chamber with internal fluid circulation (EM-CSYS-8, Physiologic Instruments). The apical and basolateral compartments were filled with a solution containing 126 mM NaCl, 0.38 mM KH_2PO_4, 2.13 mM K_2HPO_4, 1 mM $CaCl_2$, 1 mM $MgSO_4$, 24 mM $NaHCO_3$, 10 mM glucose, and phenol red. Solution were continuously bubbled with a mixture of 5% CO_2-95% air and kept at 37°C. The transepithelial voltage was clamped at 0 mV with an eight-channel voltage-clamp amplifier (VCC MC8, Physiologic Instruments, San Diego, CA, USA) connected to apical and basolateral compartments with Ag/AgCl electrodes through agar bridges (1 M KCl in 2% agar). The resulting short-circuit current was recorded on a personal computer with the Acquire & Analize 2.3 software (Physiologic Instruments, San Diego, CA, USA). During experiments, epithelia were sequentially treated with amiloride (10 μM, apical) to block ENaC-dependent current, CPT-cAMP (100 μM, apical and basolateral) to maximally stimulate CFTR activity, and $CFTR_{inh}$-172 (20 μm, apical) to fully inhibit CFTR.

Statistical analysis

All statistics were calculated using GraphPad Prism. For organoids and primary epithelial cell experiments, ordinary one-way analysis of variance (ANOVA) was performed followed by Tukey's multiple comparison test, with a single pooled variance. Statistical significance was defined as *p < 0.05, **p < 0.01, ***p < 0.001, ****p < 0.0001, and ns, non-significant.

DATA AND MATERIALS AVAILABILITY

GUIDE-seq and targeted deep-sequencing data have been deposited at BioProject (https://www.ncbi.nlm.nih.gov/bioproject/) under the accession number PRJNA895214. All other relevant data are available from the authors upon request.

SUPPLEMENTAL INFORMATION

Supplemental information can be found online at https://doi.org/10.1016/j.ymthe.2023.03.004.

ACKNOWLEDGMENTS

The authors are grateful to lab members of Cereseto lab for helpful discussion throughout the project and to Alice Setti for technical support. We wish to thank the LaBSSAH-CIBIO Next Generation Sequencing Facility of the University of Trento for sequencing samples and technical support. We are grateful to the Primary Cell Culture Service of the Italian Cystic Fibrosis Research Foundation at the Laboratory of Medical Genetics, G. Gaslini Institute, Genova, Italy, for CF primary cells.

This work was supported by the Italian Cystic Fibrosis Research Foundation grants FFC#3/2019 (adopted by Delegazione FFC di Vercelli, Delegazione FFC di Verona Val d'Alpone, Associazione Trentina Fibrosi Cistica in ricordo di Marco Menegus, Delegazione FFC di Olbia), FFC#2/2021 (adopted by Together for Life 2021), and the European Union's Horizon 2020 innovation program through the Unlocking Precision Gene Therapy (UPGRADE) project (grant agreement no. 825825).

AUTHOR CONTRIBUTIONS

A.C. and G.M. designed research. S.A. performed most experiments. M.C. analyzed the GUIDE-seq and NGS results. M.M.E. and L.DK. performed experiments and functional analysis in intestinal organoids. D.G. performed Ussing chamber experiments in primary BE cells. A.C., G.M., and S.A. wrote the manuscript. D.G., M.M.E., A.S.R., L.J.V.G., and M.S.C. reviewed the manuscript. All authors read and approved the final manuscript.

DECLARATION OF INTERESTS

A.C. is a co-founder and holds stocks of Alia Therapeutics, a genome editing company.

REFERENCES

1. Ratjen, F., Bell, S.C., Rowe, S.M., Goss, C.H., Quittner, A.L., and Bush, A. (2015). Cystic fibrosis. Nat. Rev. Dis. Primers *1*, 15010. https://doi.org/10.1038/nrdp.2015.10.

2. Shteinberg, M., Haq, I.J., Polineni, D., and Davies, J.C. (2021). Cystic fibrosis. Lancet *397*, 2195–2211. https://doi.org/10.1016/S0140-6736(20)32542-3.

3. Lopes-Pacheco, M. (2019). CFTR modulators: the changing face of cystic fibrosis in the era of precision medicine. Front. Pharmacol. *10*, 1662. https://doi.org/10.3389/fphar.2019.01662.

4. Volkova, N., Moy, K., Evans, J., Campbell, D., Tian, S., Simard, C., Higgins, M., Konstan, M.W., Sawicki, G.S., Elbert, A., et al. (2020). Disease progression in patients

with cystic fibrosis treated with ivacaftor: data from national US and UK registries. J. Cyst. Fibros. *19*, 68–79. https://doi.org/10.1016/j.jcf.2019.05.015.

5. Taylor-Cousar, J.L., Mall, M.A., Ramsey, B.W., McKone, E.F., Tullis, E., Marigowda, G., McKee, C.M., Waltz, D., Moskowitz, S.M., Savage, J., et al. (2019). Clinical development of triple-combination CFTR modulators for cystic fibrosis patients with one or two F508del alleles. ERJ Open Res. *5*, 00082-2019. https://doi.org/10.1183/23120541.00082-2019.

6. McNamara, J.J., McColley, S.A., Marigowda, G., Liu, F., Tian, S., Owen, C.A., Stiles, D., Li, C., Waltz, D., Wang, L.T., and Sawicki, G.S. (2019). Safety, pharmacokinetics, and pharmacodynamics of lumacaftor and ivacaftor combination therapy in children aged 2–5 years with cystic fibrosis homozygous for F508del-CFTR: an open-label phase 3 study. Lancet Respir. Med. *7*, 325–335. https://doi.org/10.1016/S2213-2600(18)30460-0.

7. Davies, J.C., Cunningham, S., Harris, W.T., Lapey, A., Regelmann, W.E., Sawicki, G.S., Southern, K.W., Robertson, S., Green, Y., Cooke, J., et al. (2016). Safety, pharmacokinetics, and pharmacodynamics of ivacaftor in patients aged 2–5 years with cystic fibrosis and a CFTR gating mutation (KIWI): an open-label, single-arm study. Lancet Respir. Med. *4*, 107–115. https://doi.org/10.1016/S2213-2600(15)00545-7.

8. Yan, Z., McCray, P.B., Jr., and Engelhardt, J.F. (2019). Advances in gene therapy for cystic fibrosis lung disease. Hum. Mol. Genet. *28*, R88–R94. https://doi.org/10.1093/hmg/ddz139.

9. Maule, G., Arosio, D., and Cereseto, A. (2020). Gene therapy for cystic fibrosis: progress and challenges of genome editing. Int. J. Mol. Sci. *21*, 3903. https://doi.org/10.3390/ijms21113903.

10. Zabner, J., Couture, L.A., Gregory, R.J., Graham, S.M., Smith, A.E., and Welsh, M.J. (1993). Adenovirus-mediated gene transfer transiently corrects the chloride transport defect in nasal epithelia of patients with cystic fibrosis. Cell *75*, 207–216. https://doi.org/10.1016/0092-8674(93)80063-K.

11. Caplen, N.J., Alton, E.W., Middleton, P.G., Dorin, J.R., Stevenson, B.J., Gao, X., Durham, S.R., Jeffery, P.K., Hodson, M.E., Coutelle, C., et al. (1995). Liposome-mediated CFTR gene transfer to the nasal epithelium of patients with cystic fibrosis. Nat. Med. *1*, 39–46. https://doi.org/10.1038/nm0195-39.

12. Zabner, J., Ramsey, B.W., Meeker, D.P., Aitken, M.L., Balfour, R.P., Gibson, R.L., Launspach, J., Moscicki, R.A., Richards, S.M., and Standaert, T.A. (1996). Repeat administration of an adenovirus vector encoding cystic fibrosis transmembrane conductance regulator to the nasal epithelium of patients with cystic fibrosis. J. Clin. Invest. *97*, 1504–1511. https://doi.org/10.1172/JCI118573.

13. Alton, E.W., Beekman, J.M., Boyd, A.C., Brand, J., Carlon, M.S., Connolly, M.M., Chan, M., Conlon, S., Davidson, H.E., Davies, J.C., et al. (2017). Preparation for a first-in-man lentivirus trial in patients with cystic fibrosis. Thorax *72*, 137–147. https://doi.org/10.1136/thoraxjnl-2016-208406.

14. Schwank, G., Koo, B.-K., Sasselli, V., Dekkers, J.F., Heo, I., Demircan, T., Sasaki, N., Boymans, S., Cuppen, E., van der Ent, C.K., et al. (2013). Functional repair of CFTR by CRISPR/Cas9 in intestinal Stem cell organoids of cystic fibrosis patients. Cell Stem Cell *13*, 653–658. https://doi.org/10.1016/j.stem.2013.11.002.

15. Firth, A.L., Menon, T., Parker, G.S., Qualls, S.J., Lewis, B.M., Ke, E., Dargitz, C.T., Wright, R., Khanna, A., Gage, F.H., and Verma, I.M. (2015). Functional gene correction for cystic fibrosis in lung epithelial cells generated from patient iPSCs. Cell Rep. *12*, 1385–1390. https://doi.org/10.1016/j.celrep.2015.07.062.

16. Hollywood, J.A., Lee, C.M., Scallan, M.F., and Harrison, P.T. (2016). Analysis of gene repair tracts from Cas9/gRNA double-stranded breaks in the human CFTR gene. Sci. Rep. *6*, 32230. https://doi.org/10.1038/srep32230.

17. Ruan, J., Hirai, H., Yang, D., Ma, L., Hou, X., Jiang, H., Wei, H., Rajagopalan, C., Mou, H., Wang, G., et al. (2019). Efficient gene editing at major CFTR mutation loci. Mol. Ther. Nucleic Acids *16*, 73–81. https://doi.org/10.1016/j.omtn.2019.02.006.

18. Vaidyanathan, S., Salahudeen, A.A., Sellers, Z.M., Bravo, D.T., Choi, S.S., Batish, A., Le, W., Baik, R., de la O, S., Kaushik, M.P., et al. (2020). High-efficiency, selection-free gene repair in airway Stem cells from cystic fibrosis patients rescues CFTR function in differentiated epithelia. Cell Stem Cell *26*, 161–171.e4. https://doi.org/10.1016/j.stem.2019.11.002.

19. Suzuki, S., Crane, A.M., Anirudhan, V., Barillà, C., Matthias, N., Randell, S.H., Rab, A., Sorscher, E.J., Kerschner, J.L., Yin, S., et al. (2020). Highly efficient gene editing of cystic fibrosis patient-derived airway basal cells results in functional CFTR correction. Mol. Ther. *28*, 1684–1695. https://doi.org/10.1016/j.ymthe.2020.04.021.

20. Sanz, D.J., Hollywood, J.A., Scallan, M.F., and Harrison, P.T. (2017). Cas9/gRNA targeted excision of cystic fibrosis-causing deep-intronic splicing mutations restores normal splicing of CFTR mRNA. PLOS ONE *12*, e0184009. https://doi.org/10.1371/journal.pone.0184009.

21. Maule, G., Casini, A., Montagna, C., Ramalho, A.S., De Boeck, K., Debyser, Z., Carlon, M.S., Petris, G., and Cereseto, A. (2019). Allele specific repair of splicing mutations in cystic fibrosis through AsCas12a genome editing. Nat. Commun. *10*, 3556. https://doi.org/10.1038/s41467-019-11454-9.

22. Cullot, G., Boutin, J., Toutain, J., Prat, F., Pennamen, P., Rooryck, C., Teichmann, M., Rousseau, E., Lamrissi-Garcia, I., Guyonnet-Duperat, V., et al. (2019). CRISPR-Cas9 genome editing induces megabase-scale chromosomal truncations. Nat. Commun. *10*, 1136. https://doi.org/10.1038/s41467-019-09006-2.

23. Kosicki, M., Tomberg, K., and Bradley, A. (2018). Repair of double-strand breaks induced by CRISPR–Cas9 leads to large deletions and complex rearrangements. Nat. Biotechnol. *36*, 765–771. https://doi.org/10.1038/nbt.4192.

24. Liu, Y., Ma, G., Gao, Z., Li, J., Wang, J., Zhu, X., Ma, R., Yang, J., Zhou, Y., Hu, K., et al. (2022). Global chromosome rearrangement induced by CRISPR-Cas9 reshapes the genome and transcriptome of human cells. Nucleic Acids Res. *50*, 3456–3474. https://doi.org/10.1093/nar/gkac153.

25. Leibowitz, M.L., Papathanasiou, S., Doerfler, P.A., Blaine, L.J., Sun, L., Yao, Y., Zhang, C.-Z., Weiss, M.J., and Pellman, D. (2021). Chromothripsis as an on-target consequence of CRISPR–Cas9 genome editing. Nat. Genet. *53*, 895–905. https://doi.org/10.1038/s41588-021-00838-7.

26. Adikusuma, F., Piltz, S., Corbett, M.A., Turvey, M., McColl, S.R., Helbig, K.J., Beard, M.R., Hughes, J., Pomerantz, R.T., and Thomas, P.Q. (2018). Large deletions induced by Cas9 cleavage. Nature *560*, E8–E9. https://doi.org/10.1038/s41586-018-0380-z.

27. Komor, A.C., Kim, Y.B., Packer, M.S., Zuris, J.A., and Liu, D.R. (2016). Programmable editing of a target base in genomic DNA without double-stranded DNA cleavage. Nature *533*, 420–424. https://doi.org/10.1038/nature17946.

28. Gaudelli, N.M., Komor, A.C., Rees, H.A., Packer, M.S., Badran, A.H., Bryson, D.I., and Liu, D.R. (2017). Programmable base editing of A•T to G•C in genomic DNA without DNA cleavage. Nature *551*, 464–471. https://doi.org/10.1038/nature24644.

29. Anzalone, A.V., Randolph, P.B., Davis, J.R., Sousa, A.A., Koblan, L.W., Levy, J.M., Chen, P.J., Wilson, C., Newby, G.A., Raguram, A., and Liu, D.R. (2019). Search-and-replace genome editing without double-strand breaks or donor DNA. Nature *576*, 149–157. https://doi.org/10.1038/s41586-019-1711-4.

30. (2011). The Clinical and Functional TRanslation of CFTR (CFTR2) (US CF Foundation, Johns Hopkins University, The Hospital for Sick Children). http://cftr2.org.

31. Mention, K., Santos, L., and Harrison, P.T. (2019). Gene and base editing as a therapeutic option for cystic fibrosis—learning from other diseases. Genes *10*, 387. https://doi.org/10.3390/genes10050387.

32. Geurts, M.H., de Poel, E., Amatngalim, G.D., Oka, R., Meijers, F.M., Kruisselbrink, E., van Mourik, P., Berkers, G., de Winter-de Groot, K.M., Michel, S., et al. (2020). CRISPR-based adenine editors correct nonsense mutations in a cystic fibrosis organoid biobank. Cell Stem Cell *26*, 503–510.e7. https://doi.org/10.1016/j.stem.2020.01.019.

33. Jiang, T., Henderson, J.M., Coote, K., Cheng, Y., Valley, H.C., Zhang, X.-O., Wang, Q., Rhym, L.H., Cao, Y., Newby, G.A., et al. (2020). Chemical modifications of adenine base editor mRNA and guide RNA expand its application scope. Nat. Commun. *11*, 1979. https://doi.org/10.1038/s41467-020-15892-8.

34. Krishnamurthy, S., Traore, S., Cooney, A.L., Brommel, C.M., Kulhankova, K., Sinn, P.L., Newby, G.A., Liu, D.R., and McCray, P.B. (2021). Functional correction of *CFTR* mutations in human airway epithelial cells using adenine base editors. Nucleic Acids Res. *49*, 10558–10572. https://doi.org/10.1093/nar/gkab788.

35. Duguépéroux, I., and De Braekeleer, M. (2005). The CFTR 3849+10kbC->T and 2789+5G->A alleles are associated with a mild CF phenotype. Eur. Respir. J. *25*, 468–473. https://doi.org/10.1183/09031936.05.10100004.

36. Masvidal, L., Igreja, S., Ramos, M.D., Alvarez, A., de Gracia, J., Ramalho, A., Amaral, M.D., Larriba, S., and Casals, T. (2014). Assessing the residual CFTR gene expression in human nasal epithelium cells bearing CFTR splicing mutations causing cystic fibrosis. Eur. J. Hum. Genet. *22*, 784–791. https://doi.org/10.1038/ejhg.2013.238.

37. Cooper, T.A. (2005). Use of minigene systems to dissect alternative splicing elements. Methods *37*, 331–340. https://doi.org/10.1016/j.ymeth.2005.07.015.

38. Sharma, N., Sosnay, P.R., Ramalho, A.S., Douville, C., Franca, A., Gottschalk, L.B., Park, J., Lee, M., Vecchio-Pagan, B., Raraigh, K.S., et al. (2014). Experimental assessment of splicing variants using expression minigenes and comparison with in silico predictions. Hum. Mutat. *35*, 1249–1259. https://doi.org/10.1002/humu.22624.

39. Kluesner, M.G., Nedveck, D.A., Lahr, W.S., Garbe, J.R., Abrahante, J.E., Webber, B.R., and Moriarity, B.S. (2018). EditR: a method to quantify base editing from sanger sequencing. CRISPR J. *1*, 239–250. https://doi.org/10.1089/crispr.2018.0014.

40. Dekkers, J.F., Wiegerinck, C.L., de Jonge, H.R., Bronsveld, I., Janssens, H.M., de Winter-de Groot, K.M., Brandsma, A.M., de Jong, N.W.M., Bijvelds, M.J.C., Scholte, B.J., et al. (2013). A functional CFTR assay using primary cystic fibrosis intestinal organoids. Nat. Med. *19*, 939–945. https://doi.org/10.1038/nm.3201.

41. Ensinck, M., De Keersmaecker, L., Heylen, L., Ramalho, A.S., Gijsbers, R., Farré, R., De Boeck, K., Christ, F., Debyser, Z., and Carlon, M.S. (2020). Phenotyping of rare CFTR mutations reveals distinct trafficking and functional defects. Cells *9*, 754. https://doi.org/10.3390/cells9030754.

42. Ensinck, M.M., De Keersmaecker, L., Ramalho, A.S., Cuyx, S., Van Biervliet, S., Dupont, L., Christ, F., Debyser, Z., Vermeulen, F., and Carlon, M.S. (2022). Novel CFTR modulator combinations maximise rescue of G85E and N1303K in rectal organoids. ERJ Open Res. *8*. https://doi.org/10.1183/23120541.00716-2021.

43. Ramalho, A.S., Fürstová, E., Vonk, A.M., Ferrante, M., Verfaillie, C., Dupont, L., Boon, M., Proesmans, M., Beekman, J.M., Sarouk, I., et al. (2021). Correction of CFTR function in intestinal organoids to guide treatment of cystic fibrosis. Eur. Respir. J. *57*, 1902426. https://doi.org/10.1183/13993003.02426-2019.

44. Yeo, G., and Burge, C.B. (2004). Maximum Entropy modeling of short sequence motifs with applications to RNA splicing signals. J. Comput. Biol. *11*, 377–394. https://doi.org/10.1089/1066527041410418.

45. Liang, X., Potter, J., Kumar, S., Zou, Y., Quintanilla, R., Sridharan, M., Carte, J., Chen, W., Roark, N., Ranganathan, S., et al. (2015). Rapid and highly efficient mammalian cell engineering via Cas9 protein transfection. J. Biotechnol. *208*, 44–53. https://doi.org/10.1016/j.jbiotec.2015.04.024.

46. Kim, S., Kim, D., Cho, S.W., Kim, J., and Kim, J.-S. (2014). Highly efficient RNA-guided genome editing in human cells via delivery of purified Cas9 ribonucleoproteins. Genome Res. *24*, 1012–1019. https://doi.org/10.1101/gr.171322.113.

47. Scudieri, P., Caci, E., Bruno, S., Ferrera, L., Schiavon, M., Sondo, E., Tomati, V., Gianotti, A., Zegarra-Moran, O., Pedemonte, N., et al. (2012). Association of TMEM16A chloride channel overexpression with airway goblet cell metaplasia. J. Physiol. *590*, 6141–6155. https://doi.org/10.1113/jphysiol.2012.240838.

48. Scudieri, P., Musante, I., Venturini, A., Guidone, D., Genovese, M., Cresta, F., Caci, E., Palleschi, A., Poeta, M., Santamaria, F., et al. (2020). Ionocytes and CFTR chloride channel expression in normal and cystic fibrosis nasal and bronchial epithelial cells. Cells *9*, 2090. https://doi.org/10.3390/cells9092090.

49. Capurro, V., Tomati, V., Sondo, E., Renda, M., Borrelli, A., Pastorino, C., Guidone, D., Venturini, A., Giraudo, A., S, M.B., et al. (2021). Partial rescue of F508del-CFTR stability and trafficking defects by double corrector treatment. Int. J. Mol. Sci. *22*, 5262. https://doi.org/10.3390/ijms22105262.

50. Maule, G., Ensinck, M., Bulcaen, M., and Carlon, M.S. (2021). Chapter Six - rewriting CFTR to cure cystic fibrosis. In Progress in Molecular Biology and Translational Science Curing Genetic Diseases through Genome Reprogramming, G. Petris, ed. (Academic Press), pp. 185–224. https://doi.org/10.1016/bs.pmbts.2020.12.018.

51. Tsai, S.Q., Zheng, Z., Nguyen, N.T., Liebers, M., Topkar, V.V., Thapar, V., Wyvekens, N., Khayter, C., Iafrate, A.J., Le, L.P., et al. (2015). GUIDE-seq enables genome-wide profiling of off-target cleavage by CRISPR-Cas nucleases. Nat. Biotechnol. *33*, 187–197. https://doi.org/10.1038/nbt.3117.

52. Koblan, L.W., Doman, J.L., Wilson, C., Levy, J.M., Tay, T., Newby, G.A., Maianti, J.P., Raguram, A., and Liu, D.R. (2018). Improving cytidine and adenine base editors by expression optimization and ancestral reconstruction. Nat. Biotechnol. *36*, 843–846. https://doi.org/10.1038/nbt.4172.

53. Richter, M.F., Zhao, K.T., Eton, E., Lapinaite, A., Newby, G.A., Thuronyi, B.W., Wilson, C., Koblan, L.W., Zeng, J., Bauer, D.E., et al. (2020). Phage-assisted evolution of an adenine base editor with improved Cas domain compatibility and activity. Nat. Biotechnol. *38*, 883–891. https://doi.org/10.1038/s41587-020-0453-z.

54. Gaudelli, N.M., Lam, D.K., Rees, H.A., Solá-Esteves, N.M., Barrera, L.A., Born, D.A., Edwards, A., Gehrke, J.M., Lee, S.-J., Liquori, A.J., et al. (2020). Directed evolution of adenine base editors with increased activity and therapeutic application. Nat. Biotechnol. *38*, 892–900. https://doi.org/10.1038/s41587-020-0491-6.

55. Kingwell, K. (2022). Base editors hit the clinic. Nat. Rev. Drug Discov. *21*, 545–547. https://doi.org/10.1038/d41573-022-00124-z.

56. Lin, Y., Wagner, E., and Lächelt, U. (2022). Non-viral delivery of the CRISPR/Cas system: DNA *versus* RNA *versus* RNP. Biomater. Sci. *10*, 1166–1192. https://doi.org/10.1039/D1BM01658J.

57. Kwon, H., Kim, M., Seo, Y., Moon, Y.S., Lee, H.J., Lee, K., and Lee, H. (2018). Emergence of synthetic mRNA: in vitro synthesis of mRNA and its applications in regenerative medicine. Biomaterials *156*, 172–193. https://doi.org/10.1016/j.biomaterials.2017.11.034.

58. Xu, C.-F., Chen, G.-J., Luo, Y.-L., Zhang, Y., Zhao, G., Lu, Z.-D., Czarna, A., Gu, Z., and Wang, J. (2021). Rational designs of in vivo CRISPR-Cas delivery systems. Adv. Drug Deliv. Rev. *168*, 3–29. https://doi.org/10.1016/j.addr.2019.11.005.

59. Goldman, M.J., Yang, Y., and Wilson, J.M. (1995). Gene therapy in a xenograft model of cystic fibrosis lung corrects chloride transport more effectively than the sodium defect. Nat. Genet. *9*, 126–131. https://doi.org/10.1038/ng0295-126.

60. Farmen, S.L., Karp, P.H., Ng, P., Palmer, D.J., Koehler, D.R., Hu, J., Beaudet, A.L., Zabner, J., and Welsh, M.J. (2005). Gene transfer of CFTR to airway epithelia: low levels of expression are sufficient to correct Cl− transport and overexpression can generate basolateral CFTR. Am. J. Physiol. Lung Cell. Mol. Physiol. *289*, L1123–L1130. https://doi.org/10.1152/ajplung.00049.2005.

61. Zhang, L., Button, B., Gabriel, S.E., Burkett, S., Yan, Y., Skiadopoulos, M.H., Dang, Y.L., Vogel, L.N., McKay, T., Mengos, A., et al. (2009). CFTR delivery to 25% of surface epithelial cells restores normal rates of mucus transport to human cystic fibrosis airway epithelium. Plos Biol. *7*, e1000155. https://doi.org/10.1371/journal.pbio.1000155.

62. Dannhoffer, L., Blouquit-Laye, S., Regnier, A., and Chinet, T. (2009). Functional properties of mixed cystic fibrosis and normal bronchial epithelial cell cultures. Am. J. Respir. Cell Mol. Biol. *40*, 717–723. https://doi.org/10.1165/rcmb.2008-0018OC.

63. Petris, G., Casini, A., Montagna, C., Lorenzin, F., Prandi, D., Romanel, A., Zasso, J., Conti, L., Demichelis, F., and Cereseto, A. (2017). Hit and go CAS9 delivered through a lentiviral based self-limiting circuit. Nat. Commun. *8*, 15334. https://doi.org/10.1038/ncomms15334.

64. Bloh, K., Kanchana, R., Bialk, P., Banas, K., Zhang, Z., Yoo, B.-C., and Kmiec, E.B. (2021). Deconvolution of complex DNA repair (DECODR): establishing a novel deconvolution algorithm for comprehensive analysis of CRISPR-edited sanger sequencing data. CRISPR J. *4*, 120–131. https://doi.org/10.1089/crispr.2020.0022.

65. Nobles, C.L., Reddy, S., Salas-McKee, J., Liu, X., June, C.H., Melenhorst, J.J., Davis, M.M., Zhao, Y., and Bushman, F.D. (2019). iGUIDE: an improved pipeline for analyzing CRISPR cleavage specificity. Genome Biol. *20*, 14. https://doi.org/10.1186/s13059-019-1625-3.

66. Bae, S., Park, J., and Kim, J.-S. (2014). Cas-OFFinder: a fast and versatile algorithm that searches for potential off-target sites of Cas9 RNA-guided endonucleases. Bioinformatics *30*, 1473–1475. https://doi.org/10.1093/bioinformatics/btu048.

67. Clement, K., Rees, H., Canver, M.C., Gehrke, J.M., Farouni, R., Hsu, J.Y., Cole, M.A., Liu, D.R., Joung, J.K., Bauer, D.E., and Pinello, L. (2019). CRISPResso2 provides accurate and rapid genome editing sequence analysis. Nat. Biotechnol. *37*, 224–226. https://doi.org/10.1038/s41587-019-0032-3.

68. Vonk, A.M., van Mourik, P., Ramalho, A.S., Silva, I.A.L., Statia, M., Kruisselbrink, E., Suen, S.W.F., Dekkers, J.F., Vleggaar, F.P., Houwen, R.H.J., et al. (2020). Protocol for application, standardization and validation of the forskolin-induced swelling assay in cystic fibrosis human colon organoids. STAR Protoc. *1*, 100019. https://doi.org/10.1016/j.xpro.2020.100019.

69. Mou, H., Vinarsky, V., Tata, P.R., Brazauskas, K., Choi, S.H., Crooke, A.K., Zhang, B., Solomon, G.M., Turner, B., Bihler, H., et al. (2016). Dual SMAD signaling inhibition enables long-term expansion of diverse epithelial basal cells. Cell Stem Cell *19*, 217–231. https://doi.org/10.1016/j.stem.2016.05.012.